Emerging Imaging Technologies and Techniques

17

Kang Kim, Vladimir Egorov, and S. Abbas Shobeiri

Learning Objective

1. To learn the conceptual framework for shear wave elastography
2. To learn the conceptual framework for photoacoustic imaging
3. To understand the emerging field of vaginal tactile imaging

Ultrasound Elasticity Imaging

Since it was introduced in the early 1990s as a noninvasive tool to assess the tissue mechanical properties [1–3], ultrasound elasticity imaging, also known as ultrasound elastography or sono-elastography, has been widely used in pre-clinical and clinical settings [4–14]. In clinics, elastography is intended to yield additional visual and clinically valuable information of compliance overlaid on gray-scale B-mode morphological images.

Ultrasound elasticity imaging technologies have been applied on female reproductive systems.

Freehand ultrasound real-time elastography (RTE) was used in a pilot study in 12 healthy pregnant women who underwent transvaginal ultrasound. RTE was performed by applying light repetitive compression with the hand-held vaginal transducer over the area of interest. During this palpation procedure, real-time elastogram overlaid on B-mode image and full B-mode image were displayed side by side on the screen (Fig. 17.1), resulting in easy correlation between elasticity by color distribution and the anatomical structures. A general trend of overall increased elasticity of the cervix was found in this study with a limited number of subjects [15].

In the study conducted by Swiatkowska-Freund et al., 29 women who underwent term labor induction were evaluated by elastography. The cervix was scanned while being mildly compressed with the ultrasound probe. They reported a significant difference in mean elastography index of the internal os between the patients with successful induction and those with failed induction. On the other hand, tissues near the external os and the middle of the canal did not show similar trends. The authors observed that

K. Kim
Medicine and Heart and Vascular Institute, University of Pittsburgh Medical Center, Pittsburgh, PA, USA

University of Pittsburgh School of Medicine, Pittsburgh, PA, USA

V. Egorov
Technology Development, ARTANN Laboratories, Inc, West Trenton, NJ, USA

S. Abbas Shobeiri (✉)
Department of Obstetrics and Gynecology, Gynecologic Subspecialties, INOVA Women's Hospital, Virginia Commonwealth University, 3300 Gallows Road, Second Floor South Tower, Falls Church, VA 22042-3307, USA

Department of Bioengineering, George Mason University, Fairfax, VA 22030, USA
e-mail: Abbas.shobeiri@inova.org

S. Abbas Shobeiri (ed.), *Practical Pelvic Floor Ultrasonography*, DOI 10.1007/978-3-319-52929-5_17

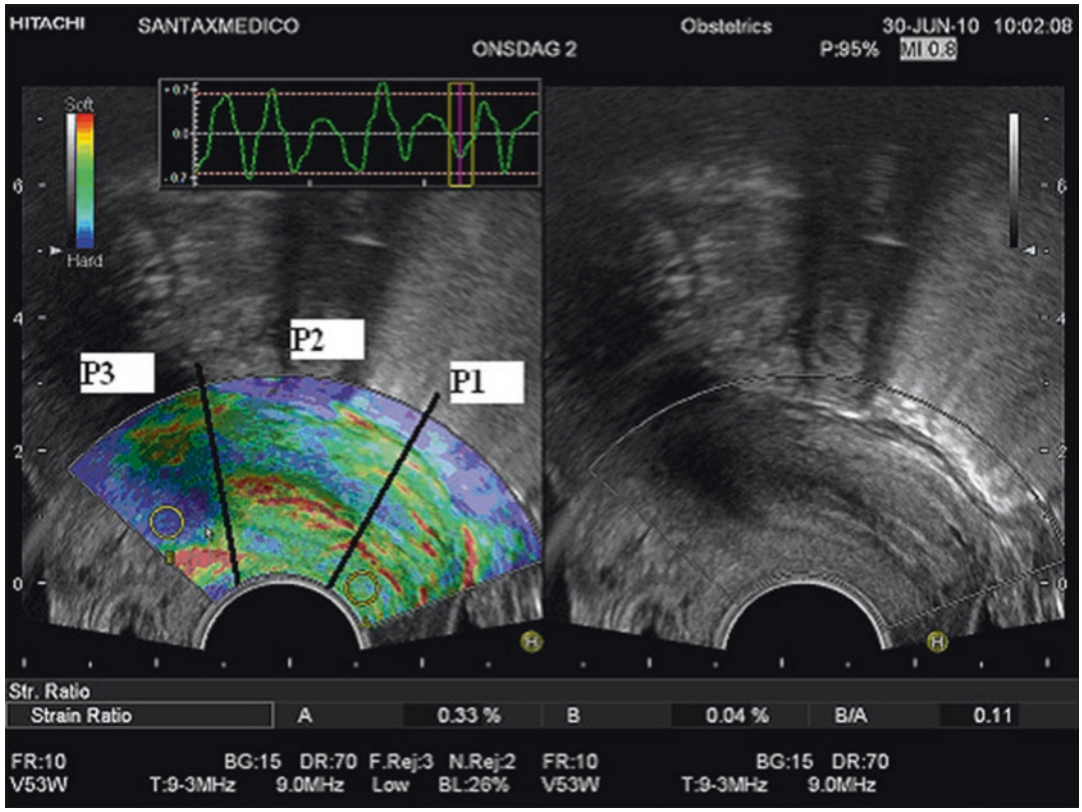

Fig. 17.1 The B-mode image (*right panel*) and the elastogram (*color*) overlaid on B-mode image (*left panel*) were displayed side by side. Lower part P1, middle part P2, upper part P3 (about one-third each) and the cervical channel. The strain ratio (*left*) in P1 is higher than the strain rate (*right*) in P3, which corresponds to the color distribution. (From Khalil et al. [15], with permission)

elastography "may guide decisions about need for cervical ripening before labor induction," noting that "the technology is limited without standardization between subjects" [16, 17]. In a cross-sectional study of 112 pregnant women at all points in gestation, no statistically significant difference between cervices was found. From the noticeable strain readings in the area where the compression was directly received, the authors addressed concerns that "measurements of rate-of-change in tissue displacement" may be "a mere reflection of the force being applied by the transducer" and might not "reflect histological changes that could provide a measure of cervical ripening." A serious step has to be taken for standardizing compression procedures that can vary between scans and subjects before elastography can be a reliable clinical tool [17, 18]. It also should be noted that the underlying structures of women's reproductive systems are complex, making it more challenging to apply pressure in a standardized way.

Acoustic Radiation Force Impulse and Shear Wave Elasticity Imaging (ARFI and SWEI) of the Cervix and Uterus

An operator-independent method that does not require standardization would be ideal. Instead of applying compression using an ultrasound probe, acoustic radiation force due to focused ultrasound can be used for remote and controlled palpation: (1) monitoring the tissue response in displacement within the radiation force region of excitation (ROE) and generating images of relative differences in tissue stiffness (acoustic radiation

force impulse [ARFI] imaging); and (2) monitoring the speed of shear wave propagation away from the ROE to quantify tissue stiffness (shear wave elasticity imaging [SWEI]). In response to electronically controlled acoustic radiation force, the resulting tissue displacement and the shear wave propagation speed directly reflect stiffness of the underlying tissue [19]. The ability of SWEI to classify ripened versus unripened tissue samples was assessed by Carson et al. using excised human hysterectomy samples. The authors stated that "if the location is accounted for, comparisons between patients can distinguish between ripened versus unripened subjects" [20].

In their human subject study, Su et al. applied ARFI and SWEI ultrasound imaging of the uterine cervix on 58 patients with pathologically confirmed cervical cancer prior to surgery. They found a statistically significant difference between the malignant lesions (stiff) and normal cervical tissues (soft). With relatively high sensitivity and specificity in the evaluation of cervical cancer, the authors stated that ARFI or SWEI can be an objective method for stiffness assessment and "may have good diagnostic value in clinical applications" [21]. In a case study of two subjects with strongly suspected leiomyosarcoma and leiomyoma, Furukawa et al. reported that SWEI can be a useful method for diagnosing uterine smooth muscle tumors (Fig. 17.2) [22].

Gennisson et al. applied SWEI on the cervix and uterus of women during pregnancy, which enabled the quantification of cervix elasticity, the follow-up of uterine elasticity during contraction, and the investigation of uterine anisotropy. In their study, cervix elasticity was quantified in 20 gravid women using a 7 MHz endocavitary probe. Uterus elasticity was quantified externally on 5 patients, through the abdomen, using an 8 MHz linear probe. Changes of elasticity were monitored in real time during uterus contraction (Fig. 17.3). SWEI was performed with the same probe by assessing shear wave speed variations with respect to probe angle, which allowed the investigation of uterine anisotropy at different depths. Elasticity values during contraction were correlated to a gold standard of uterine pressure measure [23].

In the study conducted by Tanaka et al., to investigate whether baseline stiffness of the uterine corpus and cervix changed after placental delivery, SWEI was applied on 11 patients with normal vaginal delivery before, immediately after, and 1 and 2 h after placental delivery. It was found that "the stiffness of the uterine corpus significantly changed over time, although that of the uterine cervix was not significantly altered." The authors also reported that (1) "The stiffness of the uterine corpus was significantly higher immediately after and 1 and 2 h after placental delivery as compared with that before placental delivery," and (2) "The uterine corpus had a significantly higher stiffness than the uterine cervix at each of the four time points examined" [24]. While some effects due to acoustic attenuation at depth are

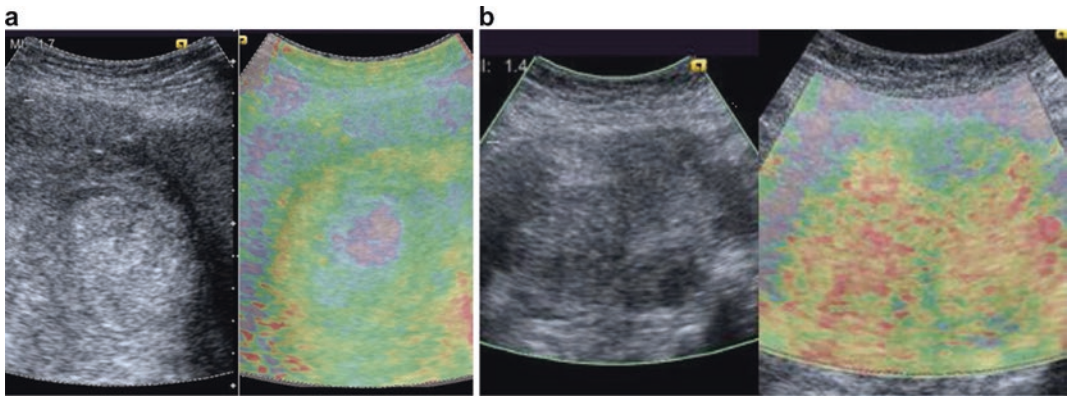

Fig. 17.2 Ultrasound images of uterine leiomyosarcoma (**a**) and leiomyoma (**b**). *Left:* Ultrasound B-mode image. *Right*: Acoustic radiation force impulse (ARFI) image. Irregular distribution of *blue*, *yellow*, *green,* and *red* was seen in the ARFI image, suggesting a heterogeneous inner structure. Notable *blue* was present in high echoic spots shown on *gray-scale* imaging. (From Furukawa et al. [22], with permission)

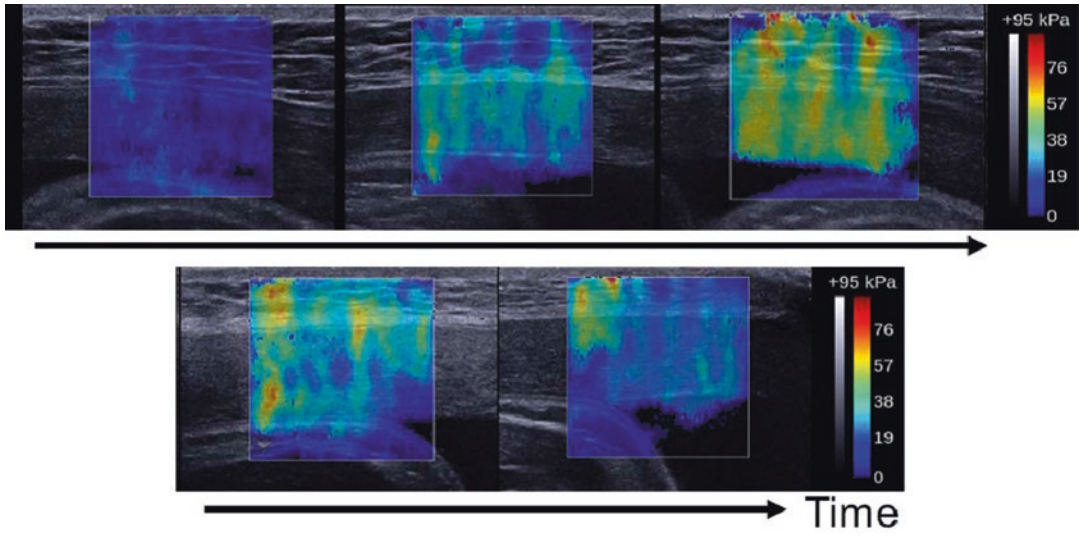

Fig. 17.3 Snapshot of the quantified elasticity map of the uterus during contraction. (From Gennisson et al. [23], with permission)

naturally expected, Hernandez-Andrade et al. demonstrated that depth from the ultrasound probe to different regions in the cervix did not significantly affect the shear wave speed estimations in the cervix of 154 pregnant women at 11–36 weeks of gestation [25].

Using tissue motion tracking methods, some important information associated with dynamic responses of the pelvic floor muscles (PFM) to potentially incontinence-producing stress, which cannot be readily captured and assimilated by the observer during the scanning process, was assessed by Peng et al. In their study, perineal ultrasonography was performed on 22 asymptomatic females and nine stress urinary incontinent (SUI) patients with a broad age distribution and parity. The ventral dorsal and cephaladcaudal movements of the anorectal angle were resolved, and kinematic parameters, in terms of displacement, trajectory, velocity, and acceleration were analyzed. The results revealed the possible mechanisms of PFM responses to prevent the urine from incontinence in fast and stress events. The statistical analyses showed the PFM responses of the healthy subjects and the SUI patients are significantly different in both the supine and standing experiments [26].

Photoacoustic Imaging of Ovarian Tissue and the Cervical Canal

Photoacoustic (PA) technology is the promising state-of-the-art medical imaging modality to provide a non-invasive quantitative optical contrast, at depth, and in real-time by using energy conversion from absorbed light energy to acoustic wave in tissue [27–29]. Salehi et al. used a hand-held transvaginal probe they designed for co-registered photoacoustic and ultrasound imaging to image ex vivo benign and malignant human ovaries (Fig. 17.4). They were able to produce co-registered images that displayed different vasculature distributions on the surface of the benign cyst and the malignant ovary [30, 31].

Using their 1.75-D array transducer, Aguirre et al. imaged normal porcine ovarian tissue as compared to histological images (see Fig. 17.4). The authors stated that their results showed excellent co-registration of ultrasound and photoacoustic images. They described strong optical absorption from vasculature, especially highly vascularized corpus luteum and low absorption from follicles [32].

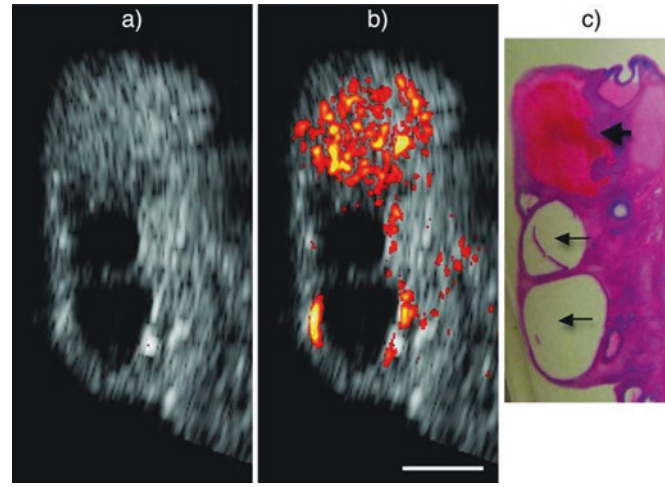

Fig. 17.4 Co-registered image of ovary 3. (**a**) Ultrasound-only image. **(b)** Photoacoustic image on top of the ultrasound image. (**c**) Hematoxylin and eosin (H&E) stained histological slide. The *white bar* represents 5 mm. (From Aguirre et al. [32], with permission)

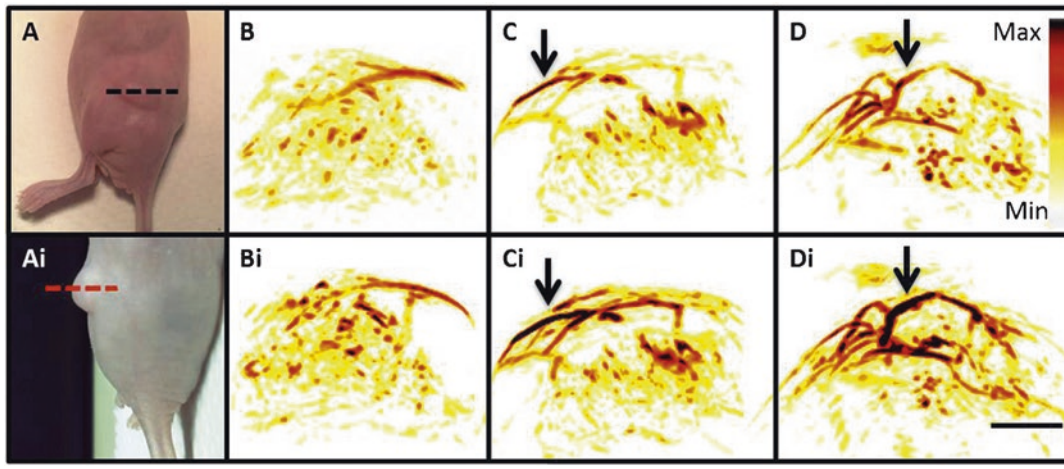

Fig. 17.5 Photoacoustic imaging of mouse tumor. *Panels A* and *Ai* are two different views of the imaging plane used to create the renderings in panels *B–D* (*dashed lines*). The top images are before injection of carbon-based nanopipettes (CNPs) and lower panels denoted by "*i*" are post-injection. *B,* no injection; *C,* 1.2 mg/mL; and *D,* 2.4 mg/mL. *Intensity bar* in *D* applies to all images, as does the *scale bar* in *Di*, which represents 3 mm. *Arrows* highlight regions with particularly increased photoacoustic contrast in post-injection images. (From Jokerst et al. [34], with permission)

Photoacoustic imaging (PAI) is sensitive to the abnormal angiogenesis deep in biological tissue, and may be capable of intact scanning both around the external orifice and in cervical canal. With this hypothesis, Peng et al. applied PAI on 30 human tissue sample harvested from the cervical canal by biopsy during a cervical colposcopical screening. They reported stronger absorption from the cervical lesions compared to normal tissue. The estimated mean optical absorption from PAI between normal tissue and cervical lesion exhibited statistically significant difference [33].

Using cellulose-based nanoparticles with a peak photoacoustic signal of 700 nm, photoacoustic imaging was applied on a mouse model of human ovarian cancer (Fig. 17.5). An obvious increase of photoacoustic signal intensity in the tumor was observed when the pre-injection images (*Panels B-D*) were compared to the post-injection (*Panels Bi-Di*). Of note, the cellulose-based nanoparticles were shown to biodegrade in the presence of cellulose, a naturally occurring enzyme, indicating important advantages for clinical translation [34].

Tactile Imaging of the Female Pelvic Floor

At the end of the last century, a technology named elastography, or elasticity imaging (EI), for measuring and visualizing soft tissue viscoelastic characteristics, emerged and the ancient art of palpation gained new life [35]. The areas of applications of EI in medical diagnostics and treatment monitoring are steadily expanding. It has been shown that the elasticity of soft tissue is highly sensitive to its structure and conditions. The range of variation of the Young's modulus of soft tissues is over three orders of magnitude, from a fraction of kPa to hundreds of kPa and appears to be one of the most sensitive physical characteristics of soft tissue, yielding valuable diagnostic information [5, 36]. Many pelvic floor disorders, including prolapse, SUI, sexual dysfunction, congenital anomalies, and others, are clearly manifested in the mechanical properties of pelvic structures. Therefore, the ability of EI to map elasticity of pelvic floor opens new possibilities in the biomechanical assessment and monitoring of pelvic floor conditions [37, 38]. EI technique based on tactile imaging additionally allows measuring muscle contraction capability.

Tactile imaging (TI), also called "mechanical imaging," is a medical imaging modality that translates the sense of touch into a digital image. The tactile image is a function of $P(x,y,z)$, where P is the pressure on soft tissue surface under applied deformation, and x,y,z are coordinates where pressure P was measured [39, 40]. The tactile image is a pressure map on which the direction of tissue deformation must be specified [40].

Functional Tactile Imaging

Functional tactile imaging (FTI) is a variation of TI that translates muscle activity into a dynamic pressure pattern $P(x,y,t)$ for an area of interest, where t is time and x,y are coordinates where pressure P was measured. Muscle activity to be studied may include a voluntary contraction (e.g., a pelvic floor squeeze), an involuntary reflex contraction (e.g., due to a cough), an involuntary relaxation, or a Valsalva (veering down) maneuver [41, 42].

A vaginal tactile imaging (VTI) probe, as shown in Fig. 17.6**,** is equipped with 96 pressure (tactile) sensors laid out at every 2.5 mm along the both sides of the probe, an orientation sensor (accelerometer), and temperature sensors with micro-heaters [43]. During the clinical procedure, the probe is used to acquire pressure responses from the vaginal walls. The VTI examination procedure includes data collection from all segments of the vagina. During an examination, data are sampled from the probe sensors and displayed on the VTI monitor in real time. The resulting pressure maps (tactile images) of the vagina integrate all of the acquired pressure and positioning data for each of the pressure-sensing elements. In addition, the VTI records the dynamic contraction for pelvic floor muscles.

The Vaginal Tactile Imager, model 2S (Advanced Tactile Imaging, Artann Laboratories, West Trenton, NJ, USA), includes data analysis tools and reporting functions. It visualizes the anatomy of the vagina, incorporating spatial measurements, pressure levels, calculated pressure gradients within the pressure maps, and assesses pelvic floor muscle contraction capability (muscle strength) (Fig. 17.7). The examination procedure allows eight clinical tests (Table 17.1).

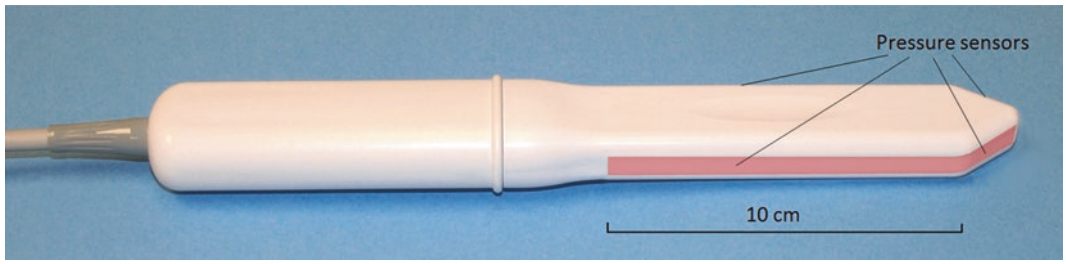

Fig. 17.6 The Vaginal Tactile Imager, model 2S (Advanced Tactile Imaging, Artann Laboratories, West Trenton, NJ, USA). Pressure sensors are aligned on the outer surface of the probe (*highlighted*)

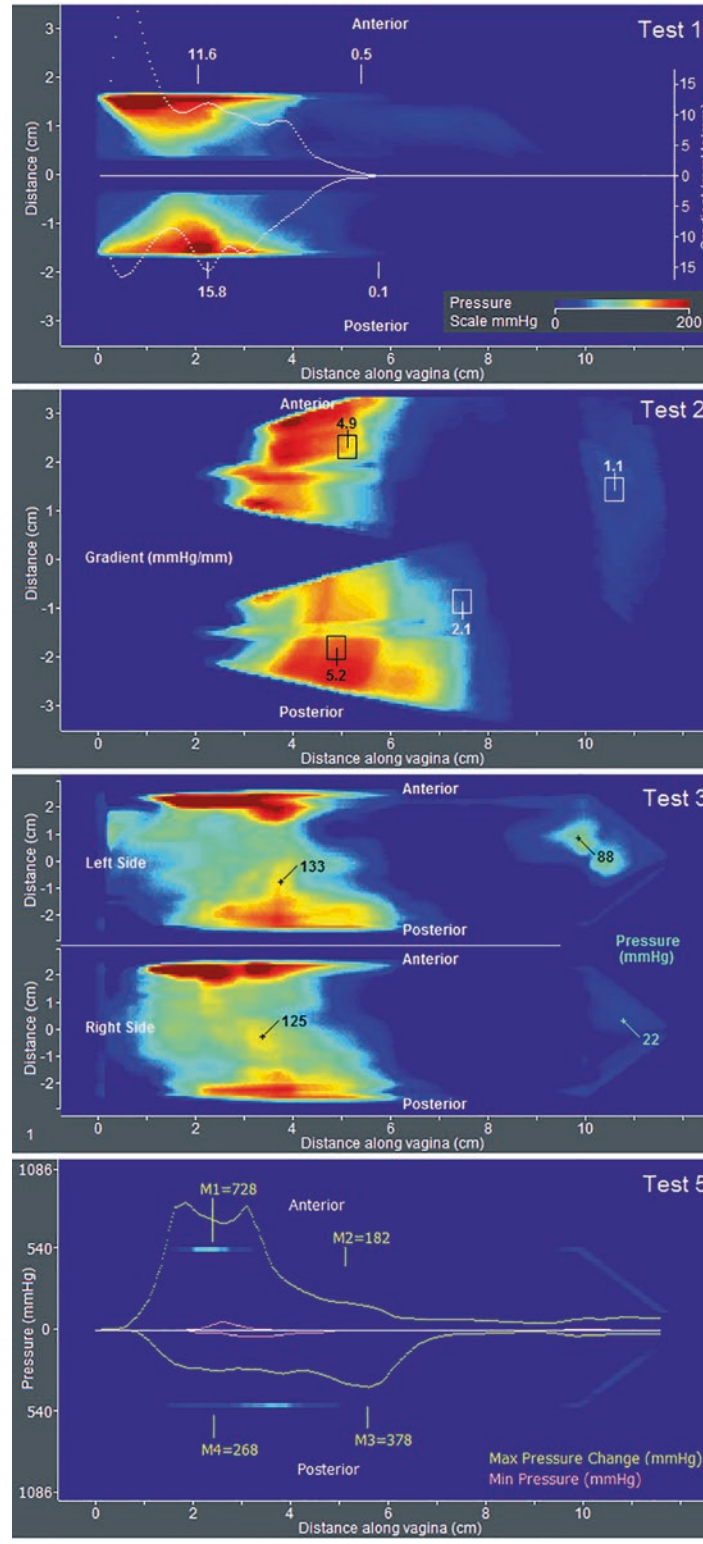

Fig. 17.7 Clinical imaging results acquired with the Vaginal Tactile Imager (Advanced Tactile Imaging, Artann Laboratories, West Trenton, NJ, USA) for 26-year-old subject with normal pelvic floor support, Test 1: Probe insertion; Test 2: Probe elevation; Test 3: Probe rotation; and Test 5: Voluntary pelvic floor muscle contraction

Table 17.1 Examination procedure and test description of the Vaginal Tactile Imager, model 2S (Advanced Tactile Imaging, Artann Laboratories, West Trenton, NJ, USA)

Test	Description
Test 1: Probe insertion	Tactile image for vaginal anterior and posterior compartments along the entire vagina; pressure gradients and anatomical sizes can be calculated
Test 2: Probe elevation	Tactile image for apical anterior and posterior compartments, relating to pelvic floor support structures; pressure gradients and anatomical sizes can be calculated
Test 3: Probe rotation	Tactile images for left and right sides of vagina (circumferential tactile image from vaginal walls); anatomical sizes can be calculated
Test 4: Valsalva maneuver	Dynamic pressure response from pelvic floor muscle contractions during Valsalva maneuver is recorded from anterior and posterior for along the entire vagina
Test 5: Voluntary muscle contraction (anterior vs. posterior)	Dynamic pressure response during voluntary pelvic floor muscle contractions is recorded from anterior and posterior along the entire vagina
Test 6: Voluntary muscle contraction (left vs. right side)	Dynamic pressure response during voluntary pelvic floor muscle contractions is recorded from left and right sides along the entire vagina
Test 7: Involuntary muscle relaxation	Dynamic pressure response during involuntary muscle relaxations is recorded from anterior and posterior along the entire vagina
Test 8: Involuntary muscle contraction	Dynamic pressure response during a cough is recorded from anterior and posterior along the entire vagina

The tactile imaging markers, sensitive to the pelvic organ prolapse (POP) conditions, were analyzed for VTI tests 1-4 (as listed in Table 17.1) in a pilot clinical study with 22 subjects [40, 43]. Nine markers were found sensitive to POP conditions ($P < 0.05$ for one-way ANOVA [analysis of variance] and/or $P < 0.05$ for t-test with correlation factor r from −0.73 to −0.56) [44, 45]. Multiple pressure peaks are observed during the pelvic floor muscle contractions. The list of markers (parameters) includes pressure, pressure gradient, and dynamic pressure response during muscle contraction at identified locations. These parameters may be used for biomechanical characterization of female pelvic floor conditions to support an effective management of pelvic floor prolapse.

The data analysis completed for VTI tests 4-8 in another clinical study with 26 subjects allowed the conclusion that pressure mapping during Valsalva maneuver, pelvic floor muscle contractions, and involuntary relaxation also may be used for quantitative characterization of POP [41]. Functional imaging of the pelvic floor muscles may offer a needed insight into the biomechanics of the functional pelvic floor to help understand the relative contribution of pelvic floor muscles in POP development and its effective treatment. Significant amplitude deference was observed in voluntary muscle contractions for the anterior vs. posterior and left vs. right side, which may allow recognition of muscle avulsion and further characterization of their functional conditions; the pressure patterns during involuntary muscle contraction (e.g., cough) are substantially different from voluntary contractions in amplitudes as well as in peak locations; patients with normal pelvic floor conditions demonstrate higher pressure applied amplitudes in both voluntary and involuntary muscle contractions than the patients with SUI; the pressure patterns during involuntary muscle contraction (cough) with SUI conditions have distinctive structure from the patterns without SUI [42].

Summary

While ultrasonography visualizes the integrity of structures and dynamics of movement, elastography and vaginal tactile imaging aim to quantify the properties of visualized structures. The ideal pelvic floor imaging modality would ultimately combine the 3D ultrasound and elastography/VTI capabilities into one single modality.

References

1. Lerner RM, Parker KJ, Holen J, Gramiak R, Waag RC. Sono-elasticity: medical elasticity images derived from ultrasound signals in mechanically vibrated targets. In: Kessler LW, editor. Acoustical imaging. Vol. 16. Proceedings of the Sixteenth International Symposium, June 10–12, 1987. New York/London:Plenum Press; 1988. p. 317–27.
2. Ophir J, Céspedes I, Ponnekanti H, Yazdi Y, Li X. Elastography: a quantitative method for imaging the elasticity of biological tissues. Ultrason Imaging. 1991;13(2):111–34.
3. Skovoroda AR, Emelianov SY, Lubinski MA, Sarvazyan AP, O'Donnell M. Theoretical analysis and verification of ultrasound displacement and strain imaging. IEEE Trans Ultrason Ferroelectr Freq Control. 1994;41(3):302–13.
4. Gao L, Parker KJ, Lerner RM, Levinson SF. Imaging of the elastic properties of tissue—a review. Ultrasound Med Biol. 1996;22(8):959–77.
5. Sarvazyan A, Hall TJ, Urban MW, Fatemi M, Aglyamov SR, Garra BS. An overview of elastography – an emerging branch of medical imaging. Curr Med Imaging Rev. 2011;7(4):255–82.
6. Zaleska-Dorobisz U, Kaczorowski K, Pawluś A, Puchalska A, Inglot M. Ultrasound elastography - review of techniques and its clinical applications. Adv Clin Exp Med. 2014;23(4):645–55.
7. Ribbers H, Lopata RG, Holewijn S, Pasterkamp G, Blankensteijn JD, de Korte CL. Noninvasive two-dimensional strain imaging of arteries: validation in phantoms and preliminary experience in carotid arteries in vivo. Ultrasound Med Biol. 2007;33(4):530–40.
8. Hall TJ, Zhu Y, Spalding CS. In vivo real-time freehand palpation imaging. Ultrasound Med Biol. 2003;29(3):427–35.
9. Kim K, Johnson LA, Jia C, Joyce JC, Rangwalla S, Higgins PDR, Rubin JM. Noninvasive ultrasound elasticity imaging (UEI) of Crohn's disease: animal model. Ultrasound Med Biol. 2008;34(6):902–12.
10. Burnside ES, Hall TJ, Sommer AM, Hesley GK, Sisney GA, Svensson WE, et al. Differentiating benign from malignant solid breast masses with US strain imaging. Radiology. 2007;245(2):401–10.
11. Luo J, Fujikura K, Homma S, Konofagou EE. Myocardial elastography at both high temporal and spatial resolution for the detection of infarcts. Ultrasound Med Biol. 2007;33(8):1206–23.
12. Rubin JM, Xie H, Kim K, Weitzel WF, Emelianov SY, Aglyamov SR, et al. Sonographic elasticity imaging of acute and chronic deep venous thrombosis in humans. J Ultrasound Med. 2006;25(9):1179–86.
13. Stidham RW, Xu J, Johnson LA, Kim K, Moons DS, McKenna BJ, et al. Ultrasound elasticity imaging for detecting intestinal fibrosis and inflammation in rats and humans with Crohn's disease. Gastroenterology. 2011;141(3):819–26.e1.
14. Weitzel WF, Kim K, Rubin JM, Wiggins RC, Xie H, Chen X, et al. Feasibility of applying ultrasound strain imaging to detect renal transplant chronic allograft nephropathy. Kidney Int. 2004;65(2):733–6.
15. Khalil MR, Thorsen P, Uldbjerg N. Cervical ultrasound elastography may hold potential to predict risk of preterm birth. Dan Med J. 2013;60(1):A4570.
16. Swiatkowska-Freund M, Preis K. Elastography of the uterine cervix: implications for success of induction of labor. Ultrasound Obstet Gynecol. 2011;38(1):52–6.
17. Feltovich H, Hall TJ, Berghella V. Beyond cervical length: emerging technologies for assessing the pregnant cervix. Am J Obstet Gynecol. 2012;207(5):345–54.
18. Molina FS, Gómez LF, Florido J, Padilla MC, Nicolaides KH. Quantification of cervical elastography: a reproducibility study. Ultrasound Obstet Gynecol. 2012;39(6):685–9.
19. Nightingale K. Acoustic radiation force impulse (ARFI) imaging: a review. Curr Med Imaging Rev. 2011;7(4):328–39.
20. Carlson LC, Feltovich H, Palmeri ML, del Rio AM, Hall TJ. Statistical analysis of shear wave speed in the uterine cervix. IEEE Trans Ultrason Ferroelectr Freq Control. 2014;61(10):1651–60.
21. Su Y, Du L, Wu Y, Zhang J, Zhang X, Jia X, et al. Evaluation of cervical cancer detection with acoustic radiation force impulse ultrasound imaging. Exp Ther Med. 2013;5(6):1715–9.
22. Furukawa S, Soeda S, Watanabe T, Nishiyama H, Fujimori K. The measurement of stiffness of uterine smooth muscle tumor by elastography. SpringerPlus 2014;3:294. doi:10.1186/2193-1801-3-294.
23. Gennisson JL, Muller M, Ami O, Kohl V, Gabor P, Musset D, Tanter M. Shear wave elastography in obstetrics: quantification of cervix elasticity and uterine contraction. In: 2011 IEEE International Ultrasonics Symposium, Orlando, FL. 2011. p. 2094–7. doi: 10.1109/ULTSYM.2011.0519. Accessed 21 Nov 2016.
24. Tanaka T, Makino S, Saito T, Yorifuji T, Koshiishi T, Tanaka S, et al. Attempt to quantify uterine involution using acoustic radiation force impulse before and after placental delivery. J Med Ultrason. 2010;38(1):21–5.
25. Hernandez-Andrade E, Aurioles-Garibay A, Garcia M, Korzeniewski SJ, Schwartz AG, Ahn H, et al. Effect of depth on shear-wave elastography estimated in the internal and external cervical os during pregnancy. J Perinat Med. 2014;42(5):549–57.
26. Peng Q, Jones R, Shishido K, Constantinou CE. Ultrasound evaluation of dynamic responses of female pelvic floor muscles. Ultrasound Med Biol. 2007;33(3):342–52.
27. Ntziachristos V. Going deeper than microscopy: the optical imaging frontier in biology. Nat Methods. 2010;7(8):603–14.

28. Emelianov SY, Li PC, O'Donnell M. Photoacoustics for molecular imaging and therapy. Phys Today. 2009;62(8):34–9.
29. Wang LV, Hu S. Photoacoustic tomography: in vivo imaging from organelles to organs. Science. 2012;335(6075):1458–62.
30. Salehi HS, Kumavor PD, Li H, Alqasemi U, Wang T, Xu C, Zhu Q. Design of optimal light delivery system for co-registered transvaginal ultrasound and photoacoustic imaging of ovarian tissue. Photoacoustics. 2015;3(3):114–22.
31. Salehi HS, Wang T, Kumavor PD, Li H, Zhu Q. Design of miniaturized illumination for transvaginal co-registered photoacoustic and ultrasound imaging. Biomed Opt Express. 2014;5(9):3074–9.
32. Aguirre A, Guo P, Gamelin J, Yan S, Sanders MM, Brewer M, Zhu Q. Coregistered three-dimensional ultrasound and photoacoustic imaging system for ovarian tissue characterization. J Biomed Opt. 2009;14(5):054014. doi:10.1117/1.3233916.
33. Peng K, He L, Wang B, Xiao J. Detection of cervical cancer based on photoacoustic imaging—the in-vitro results. Biomed Opt Express. 2014;6(i):135–43.
34. Jokerst JV, Van de Sompel D, Bohndiek SE, Gambhir SS. Cellulose nanoparticles are a biodegradable photoacoustic contrast agent for use in living mice. Photoacoustics. 2014;2(3):119–27.
35. Sarvazyan AP. Elastic properties of soft tissues. In: Levy M, Bass HE, Stern RR, editors. Handbook of elastic properties of solids, liquids and gases, vol. 3. New York: Academic Pres; 2001. p. 107–27.
36. Sarvazyan A, Egorov V. Mechanical imaging - a technology for 3-D visualization and characterization of soft tissue abnormalities: a review. Curr Med Imaging Rev. 2012;8(1):64–73.
37. Egorov V, van Raalte H, Sarvazyan A. Vaginal tactile imaging. IEEE Trans Biomed Eng. 2010;57(7):1736–44.
38. Egorov V, van Raalte H, Lucente V. Quantifying vaginal tissue elasticity under normal and prolapse conditions by tactile imaging. Int Urogynecol J. 2012;23(4):459–66.
39. Sarvazyan A. Mechanical imaging: a new technology for medical diagnostics. Int J Med Inform. 1998;49(2):195–216.
40. van Raalte H, Egorov V. Characterizing female pelvic floor conditions by tactile imaging. Int Urogynecol J. 2015;26(4): 607–9 (with video supplement).
41. van Raalte H, Lucente V, Egorov V. High definition pressure mapping of the pelvic floor muscles during Valsalva manever, voluntary muscle contraction and involuntary relaxation (abstract). In: American Urogynecologic Society 36th Annual Meeting, Seattle, WA, 13–17 Oct 2015.
42. van Raalte H, Lucente V, Egorov V. Pressure mapping of voluntary and involuntary muscle contraction for assessment of SUI conditions (abstract). In: International Continence Society 45th Annual Meeting. Montreal, Canada, 6–9 Oct 2015.
43. van Raalte H, Egorov V. Tactile imaging markers to characterize female pelvic floor conditions. Open J Obstet Gynecol. 2015;5(9):505–15.
44. Egorov V, Sarvazyan AP. Mechanical imaging of the breast. IEEE Trans Med Imaging. 2008;27(9):1275–87.
45. Egorov V, Ayrapetyan S, Sarvazyan AP. Prostate mechanical imaging: 3-D image composition and feature calculations. IEEE Trans Med Imaging. 2006;25(10):1329–40.